Precise, Efficient GPS-Based Geometric Tracking of Low Earth Orbiters

Sunil B. Bisnath and Richard B. Langley

Geodetic Research Laboratory, Department of Geodesy and Geomatics Engineering,
University of New Brunswick, Fredericton, New Brunswick, Canada.

BIOGRAPHIES

Sunil Bisnath received a B.Sc. (Hons.) in 1993 and an M.Sc. in 1995 in Surveying Science from the University of Toronto. He is currently a Ph.D. candidate in the Department of Geodesy and Geomatics Engineering at the University of New Brunswick, where he is investigating the use of GPS for precise low earth orbiter tracking.

Richard Langley is a professor in the Department of Geodesy and Geomatics Engineering at the University of New Brunswick, where he has been teaching since 1981. He has a B.Sc. in applied physics from the University of Waterloo and a Ph.D. in experimental space science from York University, Toronto. Professor Langley has been active in the development of GPS error models since the early 1980s and is a contributing editor and columnist for GPS World magazine.

ABSTRACT

Present GPS-based orbit determination techniques introduce spaceborne GPS (SGPS) receiver measurements from low earth orbiter (LEO) spacecraft into classical (dynamic) orbit determination (OD) strategies, to produce accurate *a posteriori* orbits for the LEO and the GPS constellation. A purely GPS-based tracking strategy is proposed, that does not require dynamic models and fully utilises the properties of the GPS data.

The strategy – the geometric tracking strategy – consists of applying the relative positioning technique between the LEO receiver and International GPS Service (IGS) terrestrial receivers to smooth LEO pseudorange-based position with carrier phase-based position change in a kinematic, sequential, least squares filter/smoother. The required inputs are the LEO receiver measurements, IGS precise GPS orbits, a subset of the IGS receiver network measurements, and associated station coordinate and tropospheric zenith path delay estimates.

An error propagation study was devised and carried out. Results from the study with simulated data indicate that decimetre-level position component precision can be attained. Equally-precise LEO position estimates at non-GPS measurement epochs can be computed from the filter/smoother results via interpolation. The technique promises to produce precise tracking results in only tens of minutes, regardless of LEO dynamics. Plans for future work include processing actual SGPS data, optimising and improving computer realisation of the strategy, and improving upon the interpolation algorithms.

INTRODUCTION

Accurate, time-stamped locations of earth-orbiting satellites are required for a growing number of space missions and applications, ranging from satellite altimetry to atmospheric limb sounding, to synthetic aperture radar-based imaging (see, *e.g.*, Bisnath [1999]). Traditional ground-based satellite tracking techniques are being supplemented or replaced by technologies such as GPS, where a spaceborne GPS (SGPS) receiver is placed aboard the satellite. Classical orbit determination (OD) techniques consisting of high-fidelity dynamic models utilise the GPS measurements to produce very precise orbits, *i.e.*, position with decimetre and sub-decimetre Cartesian component errors, in very complex OD strategies. See Bisnath and Langley [1999] for descriptions and comparisons of these OD strategies. However, these strategies fail to fully expolit the benefits of GPS.

In the following sections a solely GPS-based tracking strategy – the geometric tracking strategy – is proposed and described, a precision assessment is devised and carried out, conclusions are given, and plans for future research are defined.

GEOMETRIC TRACKING STRATEGY

Classical OD was designed to incorporate sparse, often imprecise measurement data that are not necessarily three-dimensional in nature. The advent of SGPS has allowed for the direct collection of continuous, accurate, three-dimensional positions. Also, in mission scenarios involving low altitudes and irregularly-shaped spacecraft, the GPS measurements can provide more accurate position estimates than the dynamic model-based strategies.

Therefore a purely geometrical, GPS-based tracking strategy is proposed, utilising only readily-available International GPS Service (IGS) data products and SGPS LEO receiver measurements. This provides for very efficient, straightforward processing and takes full advantage of the precise, three-dimensional and continuous nature of GPS measurements, as well as existing GPS data infrastructure.

A flowchart of the strategy is shown in Figure 1. The input data would be pre-processed to correct time-tags, cycle slips, *etc*. and then used to form the processing observables. The LEO position is then estimated with the filter described in the following section. By applying an accurate interpolation procedure, LEO position estimates at non-GPS measurement epochs could also be determined.

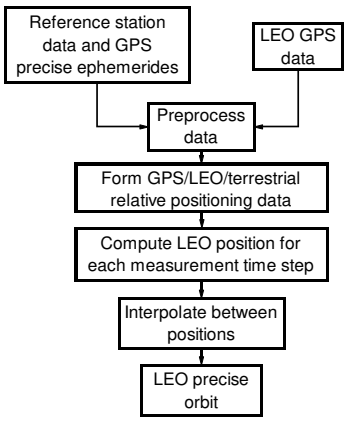

Figure 1: Flowchart of the geometric strategy.

Tracking Filter Design

The use of only GPS measurements for satellite positioning can be achieved in a number of different ways and in order of increasing position accuracy are pseudorange point positioning, pseudorange-only relative positioning from known terrestrial receiver locations, and combined pseudorange and carrier phase relative positioning. The last approach is used in this strategy and its basic form can be attributed to the seminal work of Hatch [1982]. The crux of carrier and pseudorange combination is the use of averaged noisy pseudorange range measurements to estimate the ambiguity term in the precise carrier phase range measurements. The longer the pseudorange averaging, the better the carrier ambiguity estimate.

The carrier/pseudorange averaging periods are typically short in this application due to the relatively fast motion of the LEO, necessitating frequent changing of GPS satellite-terrestrial receiver pairs. This situation does not allow for the highest precision of the technique to be attained, which calls for long averaging periods. However by performing the averaging in the *position* rather than the *range* domain, previous position solutions can be used in estimating present and future position solutions. In essence, the relative pseudoranges provide coarse position estimates and the relative carrier phase measurements provide precise position change estimates. The position change estimates are used to map all of the position estimates to one epoch for averaging.

Similar processing filters have been described by several authors including Yunck *et al.* [1986] and Kleusberg [1986]. In fact, Yunck *et al.* proposed this type of filter for the specific purpose of geometric GPS-based LEO tracking. However, this tracking strategy was abandoned for other strategies, given that poor results would be obtained since at the time sufficiently precise GPS ephemerides were not available and a global array of terrestrial GPS reference stations did not yet exist [Yunck *et al.*, 1986].

The formulation used in the present work entails differencing LEO and ground station observations between receivers, satellites, and epochs to basically remove the error effects of the GPS satellite clocks including Selective Availability (SA) (double-differencing), the GPS receiver clock errors (double-differencing), and the carrier ambiguities (triple-differencing). The use of the dual frequency observables allows for the removal of the vast majority of ionospheric effects.

Also, in an effort to mitigate data strength reduction, the LEO receiver clock was estimated in some processing tests (using between receiver single-differencing). As will be shown, the single-differencing results proved to be more precise than the double-differencing.

Filter Models and Solution

The linearised filter observation model in matrix form is

$$\begin{bmatrix} \nabla\Delta\mathbf{P}_t - \nabla\Delta\mathbf{P}_t^{\mathbf{0}} \\ \boldsymbol{\delta}\nabla\Delta\boldsymbol{\Phi}_t - \boldsymbol{\delta}\nabla\Delta\boldsymbol{\Phi}_t^{\mathbf{0}} \end{bmatrix} = \begin{bmatrix} 0 & \mathbf{A}_t \\ -\mathbf{A}_{t-1} & \mathbf{A}_t \end{bmatrix} \begin{bmatrix} \boldsymbol{\delta}\mathbf{x}_{t-1} \\ \boldsymbol{\delta}\mathbf{x}_t \end{bmatrix} + \begin{bmatrix} e_t \\ \varepsilon_{t-1,t} \end{bmatrix};$$

$$\mathbf{C}_{\nabla\Delta\mathbf{P}_t},\ \mathbf{C}_{\boldsymbol{\delta}\nabla\Delta\boldsymbol{\Phi}_t}, \qquad (1)$$

where $\nabla\Delta\mathbf{P}_t$ and $\nabla\Delta\mathbf{P}_t^{\mathbf{0}}$ are the double-differenced pseudorange measurement and approximate measurement, respectively (gives position); $\boldsymbol{\delta}\nabla\Delta\boldsymbol{\Phi}_t$ and $\boldsymbol{\delta}\nabla\Delta\boldsymbol{\Phi}_t^{\mathbf{0}}$ are the triple-differenced carrier phase measurement and approximate measurement, respectively (gives position change); $\boldsymbol{\delta}\mathbf{x}_{t-1}$ and $\boldsymbol{\delta}\mathbf{x}_t$ are the estimated corrections to the LEO position at epoch t-1 and t, respectively; $\mathbf{A}_{t-1}$ and $\mathbf{A}_t$ are the double-difference measurement partial derivatives with respect to the LEO position estimates for epochs t-1 and t, respectively; e_t and $\varepsilon_{t-1,t}$ are the measurement errors associated with $\nabla\Delta\mathbf{P}_t$ and $\boldsymbol{\delta}\nabla\Delta\boldsymbol{\Phi}_t$, respectively; and $\mathbf{C}_{\nabla\Delta\mathbf{P}_t}$ and $\mathbf{C}_{\boldsymbol{\delta}\nabla\Delta\boldsymbol{\Phi}_t}$ are the covariance matrices for $\nabla\Delta\mathbf{P}_t$ and $\boldsymbol{\delta}\nabla\Delta\boldsymbol{\Phi}_t$, respectively. Note that the undifferenced pseudorange and carrier phase measurements are assumed uncorrelated between observables and between observations. (The single-difference filter model is not shown here, but can be obtained by removing the inverted triangles and expanding the estimated corrections to include the LEO position *and* the LEO receiver clock.)

The *best* solution for (1), in a least-squares sense, is

$$\begin{bmatrix} \hat{\mathbf{x}}_{t-1} \\ \hat{\mathbf{x}}_t \end{bmatrix} = \begin{bmatrix} \mathbf{x}_{t-1}^0 \\ \mathbf{x}_t^0 \end{bmatrix} - \begin{bmatrix} \mathbf{A}_{t-1}^T\mathbf{C}_{\boldsymbol{\Phi}}^{-1}\mathbf{A}_{t-1} + \mathbf{C}_{\mathbf{x}_{t-1}}^{-1} & -\mathbf{A}_{t-1}^T\mathbf{C}_{\boldsymbol{\Phi}}^{-1}\mathbf{A}_t \\ -\mathbf{A}_t^T\mathbf{C}_{\boldsymbol{\Phi}}^{-1}\mathbf{A}_{t-1} & \mathbf{A}_t^T\left(\mathbf{C}_{\mathbf{p}}^{-1} + \mathbf{C}_{\boldsymbol{\Phi}}^{-1}\right)\mathbf{A}_t \end{bmatrix}^{-1} \times \begin{bmatrix} -\mathbf{A}_{t-1}^T\mathbf{C}_{\boldsymbol{\Phi}}^{-1}\mathbf{w}_{t-1} \\ \mathbf{A}_t^T\mathbf{C}_{\mathbf{P}}^{-1}\mathbf{w}_{t-1} + \mathbf{A}_t\mathbf{C}_{\boldsymbol{\Phi}}^{-1}\mathbf{w}_t \end{bmatrix}, \qquad (2)$$

where $\hat{\mathbf{x}} = \mathbf{x}^0 + \boldsymbol{\delta}\mathbf{x}$ (the estimate is equal to the approximate initially assumed value plus the estimated correction), $\mathbf{w}$ is the misclosure vector, and $\mathbf{C}_{\mathbf{x}_{t-1}}^{-1}$ is the LEO position covariance based on the last epoch's observations.

As can be seen, the position estimate at the previous epoch, t-1, is used to estimate the position at epoch t and so on for the moving LEO. This equation represents a kinematic sequential least-squares filter. This filter is a special case of the Kalman filter. Simply put, from (1) the pseudorange measurement contribution

$$\nabla\Delta\mathbf{P}_t - \nabla\Delta\mathbf{P}_t^{\mathbf{0}} = \mathbf{A}_t\boldsymbol{\delta}\mathbf{x}_t + e_t;$$

$$\mathbf{C}_{\nabla\Delta\mathbf{P}_t} \qquad (3)$$

can be extracted along with the carrier phase measurement contribution

$$\boldsymbol{\delta}\nabla\Delta\boldsymbol{\Phi}_t - \boldsymbol{\delta}\nabla\Delta\boldsymbol{\Phi}_t^{\mathbf{0}} = -\mathbf{A}_{t-1}\boldsymbol{\delta}\mathbf{x}_{t-1} + \mathbf{A}_t\boldsymbol{\delta}\mathbf{x}_t + \varepsilon_{t-1,t};$$
$$\mathbf{C}_{\boldsymbol{\delta}\nabla\Delta\boldsymbol{\Phi}_t}. \qquad (4)$$

The terms in (3) can be directly mapped to those of the Kalman filter measurement model, and with some rearrangement the terms in (4) can be effectively related to those of the Kalman dynamic model. That is, the kinematic sequential least-squares tracking filter behaves like a Kalman filter because the carrier phase measurements represent its dynamic model. This is illustrated heuristically in Figure 2.

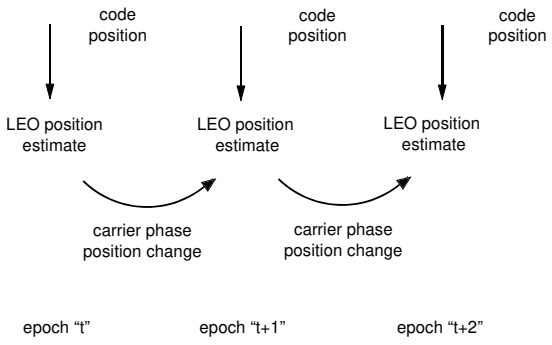

Figure 2: Combination of pseudorange and carrier phase observations in the kinematic sequential least squares filter.

Finally, since this tracking strategy is performed after-the-fact and not in real time, data smoothing can be performed. That is, the data arc can be processed in the forward and reverse directions and the results can be optimally combined. The result for the parameter covariance (see, *e.g.*, Gelb [1974]) is

$$\mathbf{C}_{\mathbf{s}_t}^{-1} = \mathbf{C}_{\mathbf{f}_t}^{-1} + \mathbf{C}_{\mathbf{r}_t}^{-1}, \qquad (5)$$

where $\mathbf{C}_{\mathbf{s}_t}$ is the smoothed parameter covariance, $\mathbf{C}_{\mathbf{f}_t}$ is the forward filter parameter covariance, and $\mathbf{C}_{\mathbf{r}_t}$ is the reverse filter parameter covariance. This is a fixed-interval smoother and as can be seen from (5), the smoothed parameter covariance is less than the results from either filter.

FILTER ERROR PROPAGATION STUDY

To determine how well this processing strategy will work, *i.e.*, with what precision can the position of the LEO receiver be determined, the covariance matrix for the estimated position unknowns is computed.

Methodology

As is well known, given the solution of a parametric least squares adjustment

$$\hat{\mathbf{x}} = \mathbf{x}^{\mathbf{0}} - \left(\mathbf{A}^{\mathrm{T}}\mathbf{P}_{\ell}\mathbf{A}\right)^{-1}\mathbf{A}^{\mathrm{T}}\mathbf{P}_{\ell}\mathbf{w}, \qquad \mathbf{P}_{\ell} = \sigma_{\mathrm{o}}^{2}\mathbf{C}_{\ell}^{-1}, \tag{6}$$

the covariance matrix for the estimated unknowns is

$$\mathbf{C}_{\hat{\mathbf{x}}} = \left(\mathbf{A}^{\mathrm{T}}\mathbf{C}_{\ell}^{-1}\mathbf{A}\right)^{-1}. \tag{7}$$

Therefore, only the mathematical model and the stochastic models of the observables are needed for this estimate and no actual measurements.

However, this estimate only contains direct measurement errors propagated through the geometry of the observing strategy. Other indirect sources of error are not included in this estimate. These two types of error are sometimes referred to as internal and external errors, respectively. In this analyses, the internal errors are the pseudorange and carrier phase measurement noise and tropospheric zenith delay residuals, and the external errors arise from GPS satellite and terrestrial reference receiver position uncertainties. $\mathrm{C}_{\hat{\mathrm{x}}}$ can be augmented to include the effects of these external errors and hence provide a larger, but *more realistic* covariance for the estimated parameters

$$\mathbf{C}'_{\hat{\mathbf{x}}} = \left(\mathbf{A}^{\mathrm{T}}\mathbf{C}_{\ell}^{-1}\mathbf{A}\right)^{-1} + \left(\mathbf{A}^{\mathrm{T}}\mathbf{C}_{\ell}^{-1}\mathbf{A}\right)^{-1}\mathbf{A}^{\mathrm{T}}\mathbf{C}_{\ell}^{-1}\mathbf{B}\mathbf{C}_{\mathbf{B}}\mathbf{B}^{\mathrm{T}}\mathbf{C}_{\ell}^{-1}\mathbf{A}\left(\mathbf{A}^{\mathrm{T}}\mathbf{C}_{\ell}^{-1}\mathbf{A}\right)^{-1}, \tag{8}$$

where $\mathbf{C}'_{\hat{\mathbf{x}}}$ is the more realistic covariance for the estimated parameters, **B** is the design matrix containing the measurement partials with respect to external error terms, and $\mathbf{C}_{\mathbf{B}}$ is the covariance matrix of the external error terms.

This procedure has been described by, *e.g.*, Strang and Borre [1997] for propagating control monument variances through geodetic network least squares adjustments. Bierman [1977] adapted the procedure for the square root information filter and refers to its use as "consider covariance analysis" based on *considering* the effects of other error sources.

Therefore, by deriving the **B** matrix and constructing the $\mathbf{C}_{\mathbf{B}}$ covariance matrix based on the given data, the precision with which the LEO receiver position can be determined for a given mission scenario can be estimated.

Mission Scenario and Data Simulation

The baseline orbit and GPS receiver used for this analysis are from the proposed tethered Canadian Bistatic Observations with Low Altitude Satellites (BOLAS) ionospheric science mission [James, 1997; Bisnath, 1997; Jablonski *et al.*, 1998] and the Allen Osborne Associates, Inc. TurboStar SGPS receiver [Kunze, 1997], respectively. BOLAS requires near-decimetre *a posteriori* satellite positions. The nominal BOLAS orbital parameters are given in Table 1. To accommodate the use of GPS on each subsatellite, it has been proposed that a 4π steradian phased antenna array be developed. In this study, the effect of using both a 2π steradian zenith-pointing antenna and a 4π steradian "full-sky" (covering both zenith and nadir hemispheres) antenna are analysed.

Orbital parameter	Value
Perigee	350 km
Apogee	780 km
Period	90 minutes
Inclination	103°
Perigee drift rate	-2.794°/day
Right ascension drift rate	1.657°/day

Table 1: Orbital parameters for the proposed BOLAS spacecraft.

The assumed input noise parameters for the study are given in Table 2. The pseudorange noise is based on a five minute integration time and the presence of Anti-Spoofing (AS). Note that the promise of new civilian GPS signals will be essentially equivalent to AS being deactivated. The remaining parameters are defined according to the International GPS Service (IGS) documentation [Neilan *et al.*, 1997; Gendt, 1998]. Note that the tropospheric error for the ground stations is mapped to the line of sight via the cosecant of the elevation angle. This is a sufficiently accurate mapping function for these preliminary studies. All signals arriving at the LEO are assumed to be free of tropospheric effects. The effects of ionospheric refraction are assumed completely removed by means of the ionosphere-free, dual frequency combination. The effect of signal multipath was not considered, but would degrade the solution if the SGPS antenna were located in a high multipath environment.

A number of variable-length simulated data sets were used with measurement integration periods ranging from 30 seconds to 300 seconds. The BOLAS ground track for the first five hours of one arc is shown in Figure 3.

Scenarios with 24, 32, and 40 globally distributed IGS ground stations were used, with ground station GPS satellite tracking elevation mask angles of 10º.

Parameter	Std. dev. (cm)
L1 pseudorange	2.2*
L2 pseudorange (AS on)	15.8*
L1 carrier phase	0.02
L2 carrier phase (AS on)	0.3
GPS precise ephemerides	5
Ground station coordinates	1
Tropospheric zenith path delay	1

Table 2: Input noise parameters for the error propagation study. *300 second integration period.

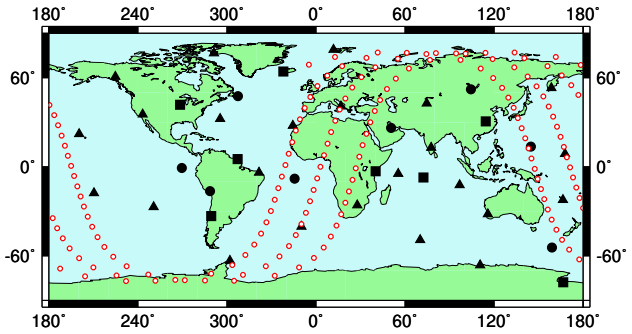

Figure 3: Example of a tracking scenario showing BOLAS ground track for a 5 hour arc. First 24 stations (>). Additional 8 stations (C). And final 8 stations (□).

Results and Analysis

In order to observe the performance and characteristics of the geometric strategy, the error propagation study was focused on the following processing parameters: data combination; number of ground stations; data arc length; measurement integration period, GPS-to-LEO signal cut-off altitude; and Anti-Spoofing (AS). Note that unless otherwise specified, the defaults for the processing parameters are: single-differencing; 32 ground stations; 6 hour data arc length, with 30 minutes removed from the tails after processing; 300 second measurement integration period; no GPS-to-LEO signal cut-off altitude; and AS active.

Figure 4 shows the effects of estimating (the bold lines) or not estimating the receiver clock. That is, single-differenced pseudoranges and double-differenced carrier phases versus double-differenced pseudoranges and triple-differenced carrier phases, respectively. The use of double-differenced observations results in (see Table 3) a mean radial component error that is more than 1 cm larger than the along-track error and more than 3 cm larger than the cross-track error. As can be seen, representing the behaviour of the LEO receiver clock with a simple white noise model, the single-differenced solution provides more precise results. The improvements are most noticeable in the radial component, which indicates almost a 1 cm improvement. This is also expected given the close relationship between receiver clock and receiver height.

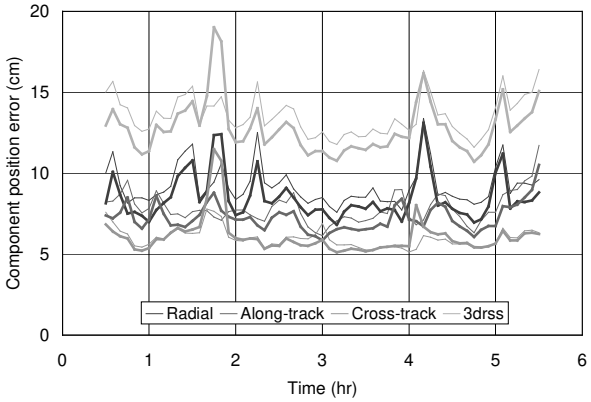

Figure 4: Effect of estimating (bold lines) and not estimating LEO receiver clock on component position error.

	d.d. processing			s.d. processing		
	Max.	Min.	Mean	Max.	Min.	Mean
Rad.	13.4	7.6	9.2	13.1	6.8	8.5
a.-t.	11.7	6.1	7.8	10.5	5.8	7.2
c.-t.	7.8	5.1	6.0	11.5	5.1	6.1
3drss	16.4	11.6	13.5	19.0	10.7	12.8

Table 3: Summary statistics (in cm) for comparison of estimating and not estimating LEO receiver clock. (rad. = radial; a.-t. = along-track; c.-t. = cross-track).

The number of ground stations using for the processing was next investigated. Given that for the simulation only one terrestrial reference station was used in the processing at each epoch, the improvement by adding ground stations was expected to be minimal. And as can be seen from Figure 5, this is the case. The improvement from 24 stations to 40 stations comes primarily in a half centimetre reduction in the radial component position error. The largest error value also does not change significantly with the varying of the number of reference stations (see Figure 6). The use of multiple reference stations is proposed for future studies.

Another processing parameter that does not have a significant effect on the position precision is the length of the data arc used in the processing. The mean position error presented in Figure 7 can be explained by the fact that the filter converges very quickly, and reaches a very

reliable steady state. However, as the data arc increases, the magnitude of the largest estimate error also increases, as can be seen in Figure 8.

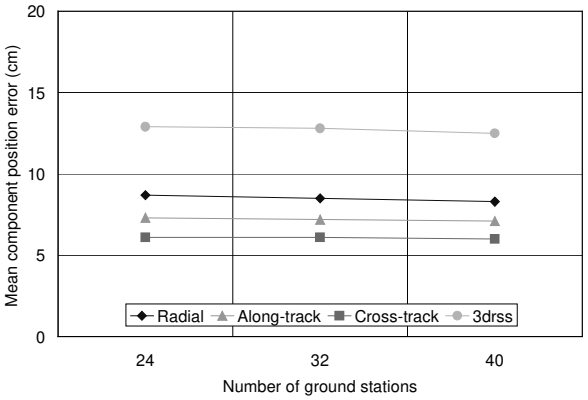

Figure 5: The effect of varying the number of ground stations on mean component position error.

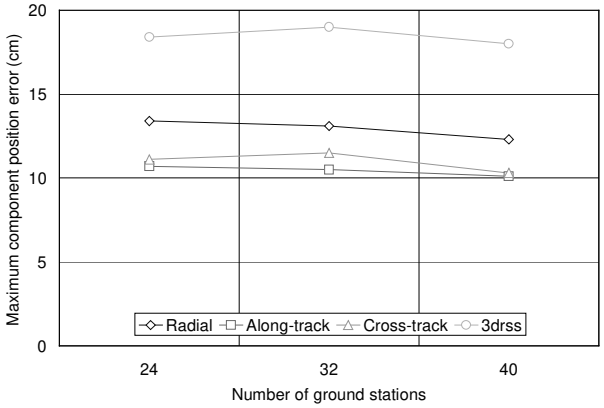

Figure 6: The effect of varying the number of ground stations on maximum component position error.

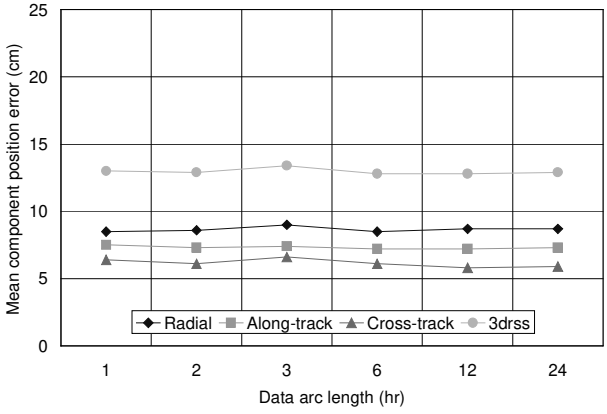

Figure 7: The effect of varying the data arc length on mean component position error.

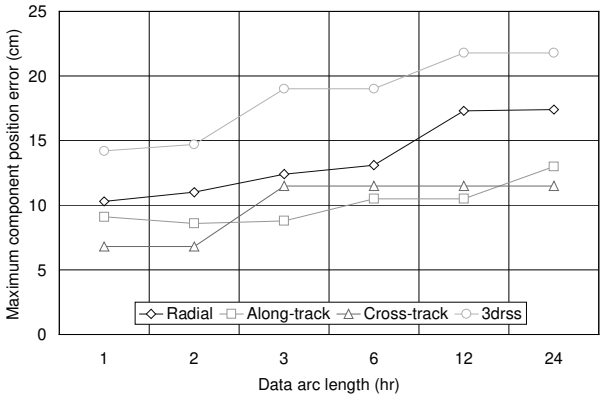

Figure 8: The effect of varying the data arc length on maximum component position error.

The LEO GPS receiver's measurement integration period plays a very important role in the final LEO position precision. This interval is inversely proportional to pseudorange variance. (One particular instance was quoted in Table 2.) Given that the pseudoranges are used to estimate the bulk of the carrier phase ambiguities, and that the precision of the pseudoranges increases with longer integration times, the larger the integration period, the more precise the resulting positions will be. Figure 9 illustrates this mapping of observable precision to position precision. For all of the position components the mean error decreases from measurement integration periods of 30 seconds to 210 seconds, and from then on the mean error remains fairly constant. As shown in Figure 10, the maximum error also decreases with increasing integration period. This implies that a measurement integration period between 210 and 300 seconds would be desirable.

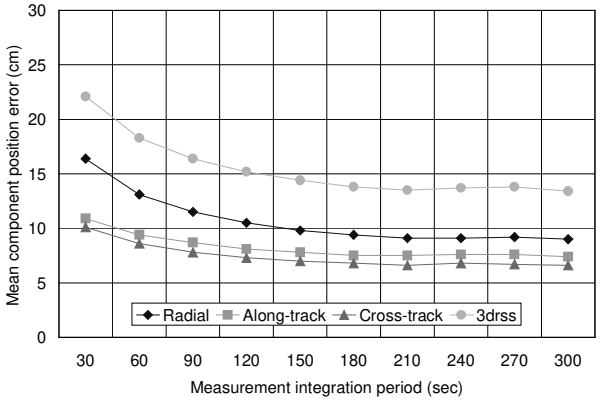

Figure 9: The effect of varying the measurement integration period on mean component position error.

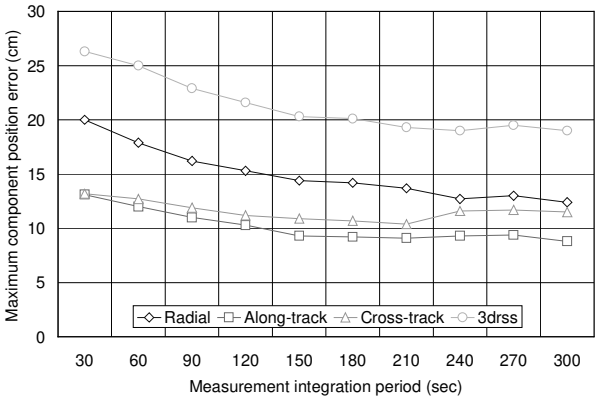

Figure 10: The effect of varying the measurement integration period on maximum component position error.

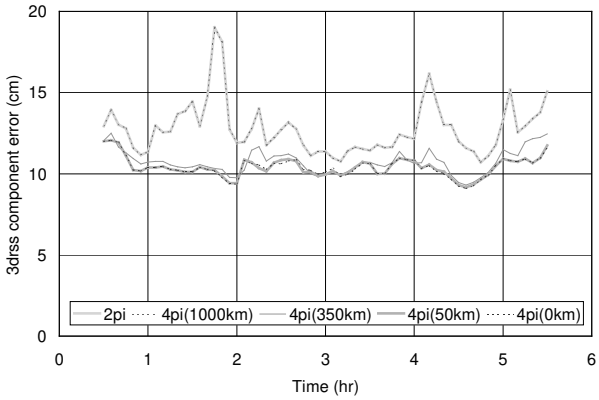

Figure 11: The effect of using a 4π steradian LEO GPS antenna on 3drss component error.

As mentioned, the BOLAS mission calls for the use of a 4π steradian LEO GPS antenna. Such an antenna will obviously improve the results of this purely geometric approach. However, the use of GPS signals that pass in and out of portions of the earth's atmosphere increases the noise in those measurements. Therefore, either these types of signals must not be used in processing, or they must be subjected to further corrections based on existing physical models. In terms of the former method, an altitude cut-off term has been created. That is, line-of-sight vectors from GPS satellites to the LEO will not be used for processing below a certain altitude threshold – the altitude cut-off.

Figure 11 compares the 2π results with a number of 4π results. Summary statistics are displayed in Table 4. For BOLAS, orbiting at relatively low altitudes, the effects of introducing a 4π steradian antenna with a 1000 km cut-off altitude is negligible compared to the zenith-hemisphere 2π steradian field-of-view antenna. However, when the cut-off is reduced to 350 km (the approximate altitude of peak ionospheric electron density) the resulting mean total displacement position noise decreases from 12.8 cm to 10.7 cm. Further reduction in the altitude cut-off to 50 and 0 km produces few millimetre improvements, indicating that the increased low elevation data provided by the longer GPS satellite data arcs does not improve the precision of the position solution.

The ideal strategy for processing actual data would therefore be to mask-out the troposphere and the lower portion of the ionosphere and, if required, to use an ionospheric model to estimate the remaining higher order ionospheric terms not accounted for in the ionospheric-free GPS combination.

LEO antenna configuration (altitude cut-off)	Mean 3drss error (cm)
2π	12.8
4π (1000 km)	12.8
4π (350 km)	10.7
4π (50 km)	10.4
4π (0 km)	10.4

Table 4: Summary statistics for 2π and 4π steradian LEO antenna comparison.

To complete this analysis, we considered the augmentation of the current GPS signal structure in the next few years which will greatly improve the precision of this tracking strategy. An indication of this can be seen when assuming AS inactive. Since AS requires civil use of the L1 pseudorange to estimate the L2 pseudorange, the removal of AS allows for much more precise L2 pseudoranges to be measured. Figure 12 compares the results with and without (bold lines) AS. The large improvement in each component (see Table 5) has mean magnitudes of 5.1 cm, 5.4 cm, and 4.2 cm in the radial, along-track and cross-track components, respectively.

	AS active			AS inactive		
	Max.	Min.	Mean	Max.	Min.	Mean
rad.	13.1	6.8	8.5	7.4	2.3	3.4
a.-t.	10.5	5.8	7.2	3.1	1.3	1.9
c.-t.	11.5	5.1	6.1	6.1	1.2	1.9
3drss	19.0	10.7	12.8	9.1	3.0	4.4

Table 5: Summary statistics (in cm) for comparison of having AS active or inactive. (rad. = radial; a.-t. = along-track; c.-t. = cross-track).

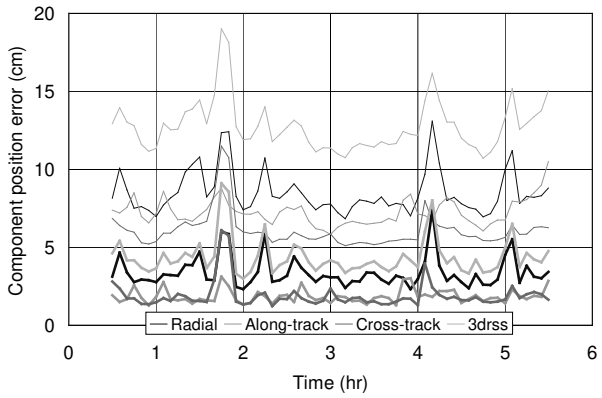

Figure 12: Effect of AS active and AS not active (bold lines) on component position error.

PRELIMINARY INTERPOLATION STUDY

In order to utilise discrete GPS-based position estimates in LEO mission applications, positions need to be accurately interpolated or approximated to epochs in-between these estimates. An initial investigation of the use of interpolation was carried out.

Methodology and Data Sets

Investigating the use of data interpolation, three parameters are of interest: the order of the interpolator, the spacing of the nodes of known functional values (in the case of the geometric tracking strategy, position estimates spaced in time as dictated by the measurement integration period), and the accuracy to which the interpolation is to be carried out. Of course, the type of interpolator has a great effect on the results of the interpolator. For this study, a 15^{th} order Lagrange interpolator was used.

A 24 hour, one second data set of the ERS2 satellite precise earth-centred, earth-fixed position estimates were used as a "truth" source. The estimates were computed with satellite laser ranging (SLR) measurements, using the GEODYN II software package with all orbit perturbations turned on. Subsets of this data set were selected (depending on the node spacing), and processed with the interpolator. The results were then differenced with the original data set to determine the accuracy of the interpolation process.

Results and Analysis

The results for interpolation node spacing of 0 seconds to 180 seconds can be seen in Figure 13. The results with spacing up to 300 seconds goes off the scale of the figure. The results have been represented in terms of the 99.73 percentile (3σ) interpolation error. That is, 0.27 percent of the errors are greater than or equal to the 3σ value. If the node interval is 90 seconds of less, basically no error is introduced in the LEO position solution due to interpolation. However, if an interval of 120 seconds is used, a small interpolator bias is introduced, particularly to the Cartesian Y position component. Using a longer node interval would produce errors at a level equal to or greater than the resulting position noise from the above processing. The use of more sophisticated interpolation or approximation procedures might improve these results.

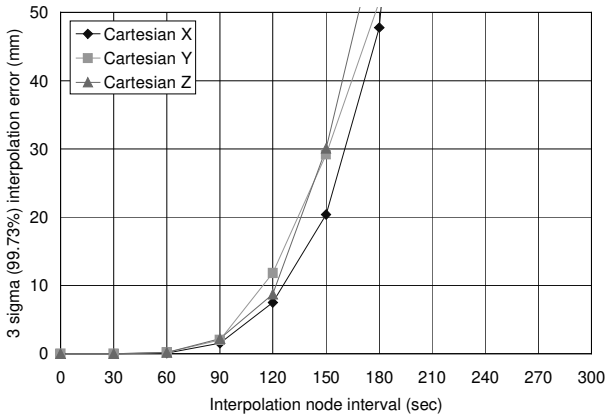

Figure 13: The effect of interpolation node interval on interpolation accuracy, for tests using ERS2 data.

FINAL RESULTS AND ANALYSIS

Given the interpolation investigation indicates that the ERS2 trajectory can be accurately interpolated from position estimates at 90 second intervals (hence a 90 second measurement integration period), Figure 14 depicts the BOLAS results of the geometric strategy for a 24 hour data arc with a measurement integration period of 90 seconds. The interpolation interval being indirectly a function of LEO altitude, an interpolation bias may be introduced for a portion of the BOLAS orbit near the perigee. 32 ground stations were used, in conjunction with a conventional 2π steradian LEO antenna and AS assumed active. This could be considered a typical processing scenario. Summary statistics are given in Table 6. From these results, it appears that equally precise positions could be interpolated using the above interpolator at other orbital points.

Component	Max. (cm)	Min. (cm)	Mean (cm)
rad.	15.5	8.7	11.3
a.-t.	14.2	6.9	8.6
c.-t.	11.0	6.0	7.3
3drss	22.6	13.8	16.0

Table 6: Summary statistics for typical position noise results from geometric strategy covariance analysis. (rad. = radial; a.-t. = along-track; c.-t. = cross-track).

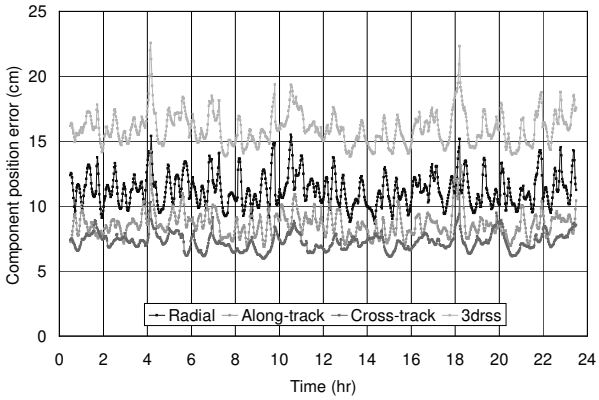

Figure 14: Typical position error results from geometric strategy covariance analysis.

Finally, Figure 15 shows the effect of each source error on the final mean LEO position error. The vast majority (approximately 90%) of the error originates from GPS receiver range measurements, regardless of the position component.

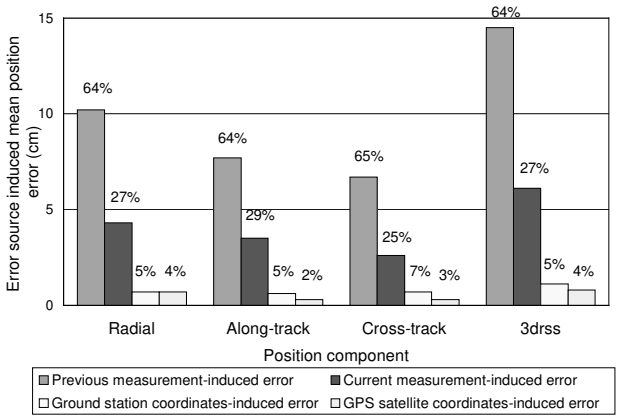

Figure 15: Geometric strategy error sources-induced mean position error.

A final comment is that the processing time required for the above scenario utilising un-optimised, uncompiled Matlab scripts on a 96 MHz MicroSPARC II was approximately 2.5 hours. Optimised, compiled code could possibly introduce a five to ten fold improvement in processing time, resulting in geometric strategy running times of only tens of minutes.

CONCLUSIONS AND FURTHER RESEARCH

A post-processing LEO tracking strategy based on GPS measurements has been proposed, which is simple and efficient. The strategy incorporates a kinematic, sequential least squares filter/smoother which utilises the full potential of the GPS measurements, and makes use of readily-available GPS-related data products. From covariance analyses, the strategy appears to provide decimetre-level positioning in each LEO Cartesian component for any instance of the LEO orbit with the aid of interpolation, and could provide this processing in only tens of minutes.

Future research includes augmenting the computer code to process *real* SGPS data, and optimising and compiling all code. The filter/smoother algorithm can be improved by, *e.g.*, utilising more than one ground station per epoch, and introducing more rigorous stochastic modelling. Finally, gains could possibly be made in interpolation accuracy or approximation could be used in its place.

ACKNOWLEDGEMENT

The authors wish to thank Dennis Gerrits, visiting researcher from the Department of Aerospace Engineering, Delft University of Technology, The Netherlands for his work in developing spacecraft-to-spacecraft visibility algorithms, and for providing the ERS2 ephemeris data.

REFERENCES

Bierman, G.J. (1977). *Factorization Methods for Discrete Sequential Estimation*. Academic Press, New York, N.Y., U.S.A., 241 pp.

Bisnath, S.B. (1997). "BOLAS Homepage." http://gauss.gge.unb.ca/BOLAS, accessed November.

Bisnath, S.B. (1999). "Spaceborne GPS information site." http://gauss.gge.unb.ca/grads/sunil/sgps.htm, accessed June.

Bisnath, S.B. and R.B. Langley (1999). "Precise *a posteriori* geometric tracking of Low Earth Orbiters with GPS," submitted to *Canadian Aeronautics and Space Journal*.

Gelb, A. (Ed.) (1974). *Applied Optimal Estimation.* Massachusetts Institute of Technology, Cambridge, Massachusetts, U.S.A., 374 pp.

Gendt, G. (1998). "IGS combination of tropospheric estimates – experience from pilot experiment." In *Proceedings of IGS 1998 Analysis Center Workshop*, Darmstadt, Germany, 9-11 February, 1998, International GPS Service, pp. 205-216.

Jablonski, A.M., H.G. James, G. Tyc, F.R. Vigneron, C.K. Carrington, C.C. Rupp, and J.K. Harrison (1998). "The BOLAS tether ionospheric mission." Paper presented at the International Academy of Astronautics Small Satellite Missions Symposium, 49th International Astronautics Federation Congress, Melbourne, Australia, 28 September - 2 October.

James, H.G. (1997). BOLAS Phase A Final Report, Report to the Canadian Space Agency, Ottawa, December.

Hatch, R. (1982), "The synergism of GPS code and carrier measurements." *Proceedings of the Third International Geodetic Symposium on Satellite Doppler Positioning*", DMA, NOS, Las Cruces, New Mexico, 8-12 February, Physical Science

Laboratory, New Mexico State University, Las Cruces, New Mexico, Vol. II, pp.1213-1232.

Kleusberg, A. (1986). "Kinematic relative positioning using GPS code and carrier beat phase observations," *Marine Geodesy*, Vol. 10, No. 3/4, pp. 257-274.

Kunze, H. (1997). Personal Communications, Allen Osborne Associates, Inc., December.

Neilan, R.E., Zumberge, J.F., Beutler, G., and Kouba, J. (1997). "The International GPS Service: A global resource for GPS applications and research." *Proceedings of the 10th International Technical Meeting of the Satellite Division of the Institute of Navigation*, Kansas City, Missouri, U.S.A., 16-19 September, 1997, The Institute of Navigation, Alexandria, Virginia, U.S.A., Vol. 1, pp. 883-889.

Strang, G. and K. Borre, (1997). *Linear Algebra, Geodesy, and GPS*. Wellesley-Cambridge Press, Wellesley, Massachusetts, U.S.A., 640 pp.

Yunck, T. P., Wu, S.-C., and Wu, J.-T. (1986). "Strategies for sub-decimeter satellite tracking with GPS," *IEEE Position, Location, and Navigation Symposium 1986*, Las Vegas, Nevada, U.S.A., 4-7 November, The Institute of Electrical and Electronics Engineers, Inc., New York, New York, U.S.A., pp. 122-128.